X–raying Active Galaxies Both Near and Far

Exploring the Environments of Supermassive Black Holes

Niel Brandt (Penn State)

Postdocs:	Dave Alexander Franz Bauer Stefan Immler	Iskra Strateva Cristian Vignali Wentao Wu
Grad. Students:	Sarah Gallagher Ann Hornschemeier	Bret Lehmer
Undergrad. Students:	Lee Bassett Matt Collinge Paul de Naray	Jennifer Donley Kevin Marshall

Many great collaborators!

Probe immediate vicinity of black hole and larger scale environment

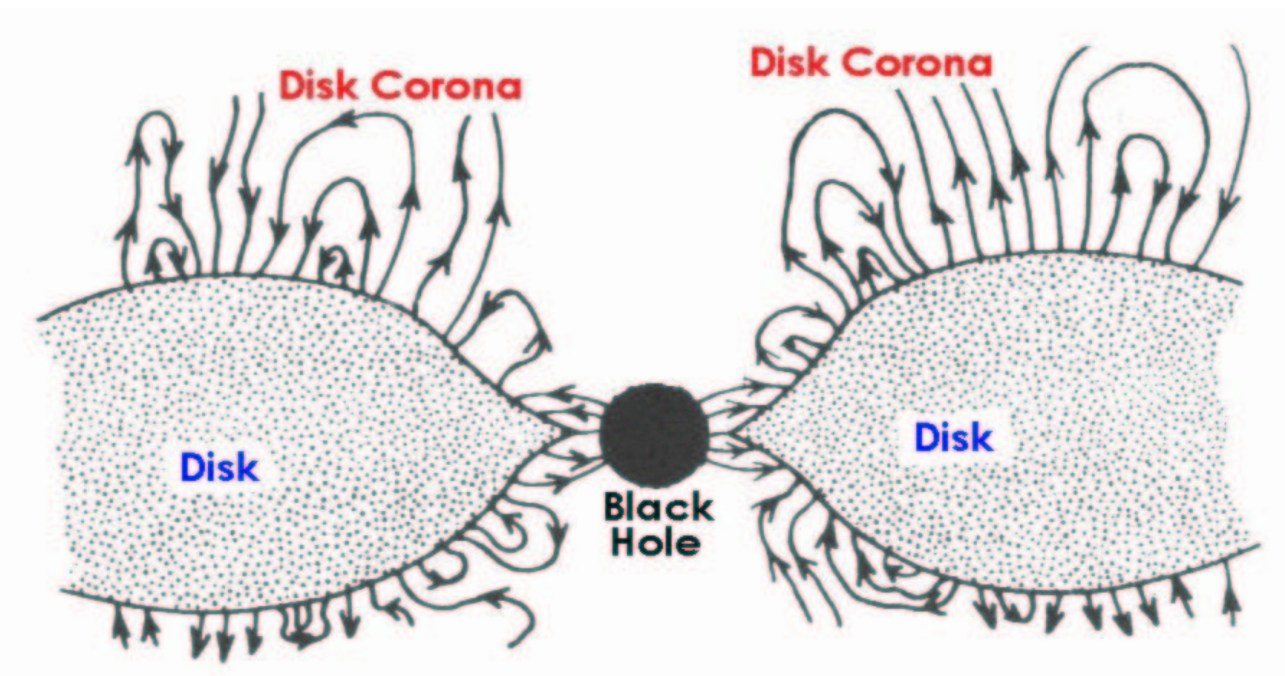

X–ray emission is a universal property of AGN

- Commonly 5–30% of total power
- When AGN are X–ray weak, mostly just absorption

Complex X–ray Spectra of Active Galaxies

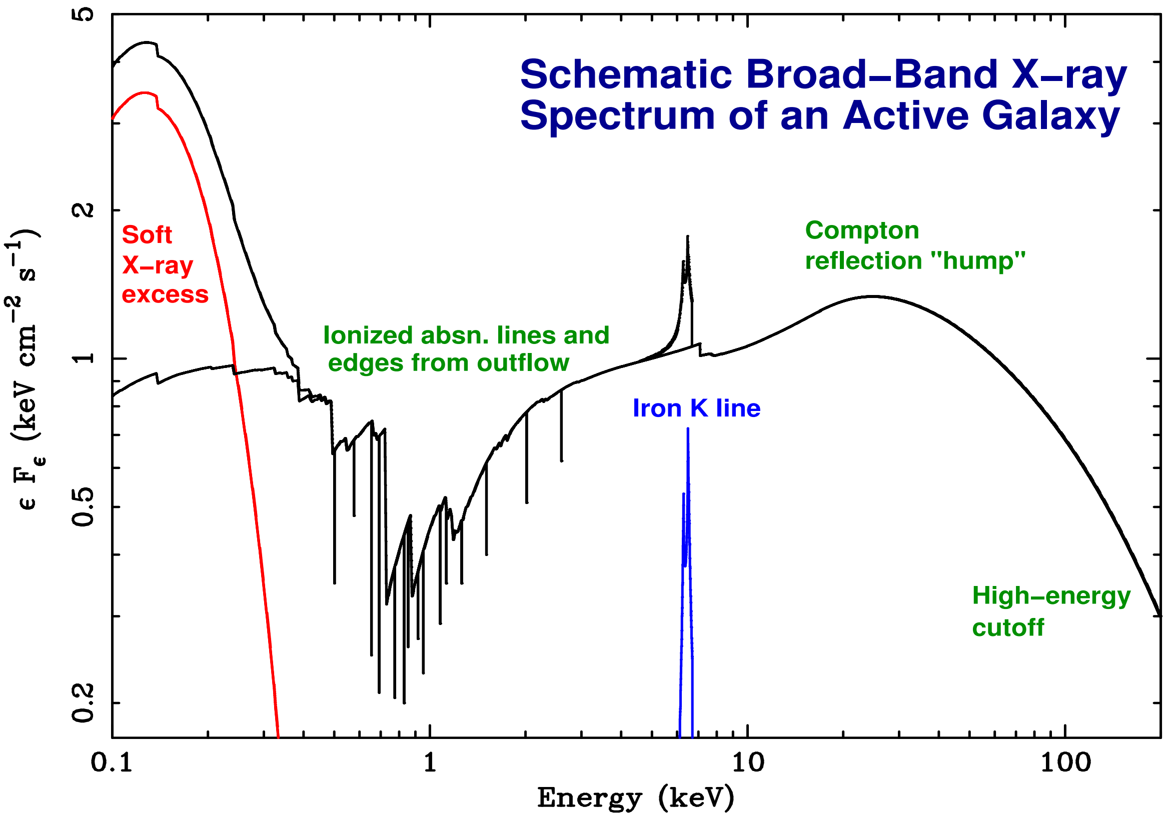

Broad bandpass, spanning factor of ~ 100–1000

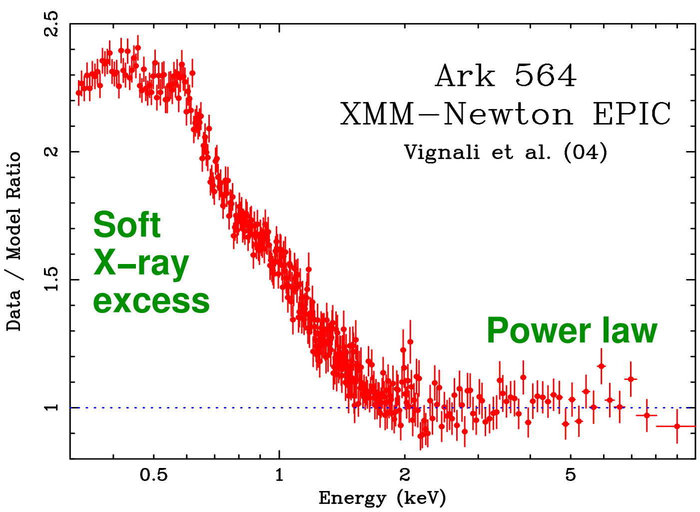

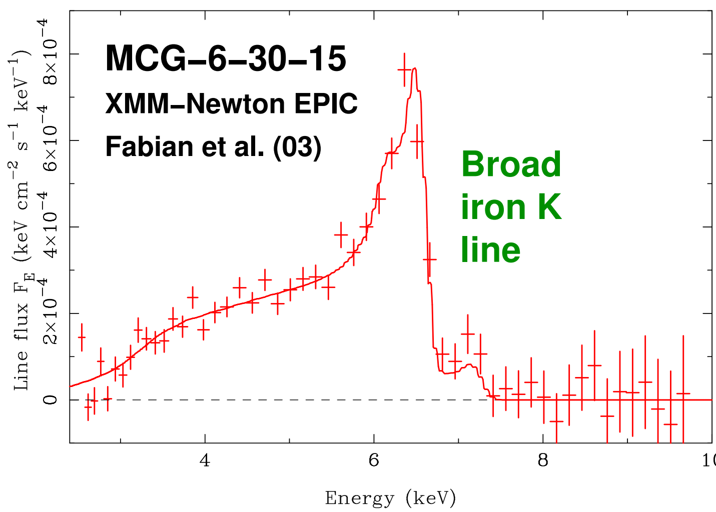

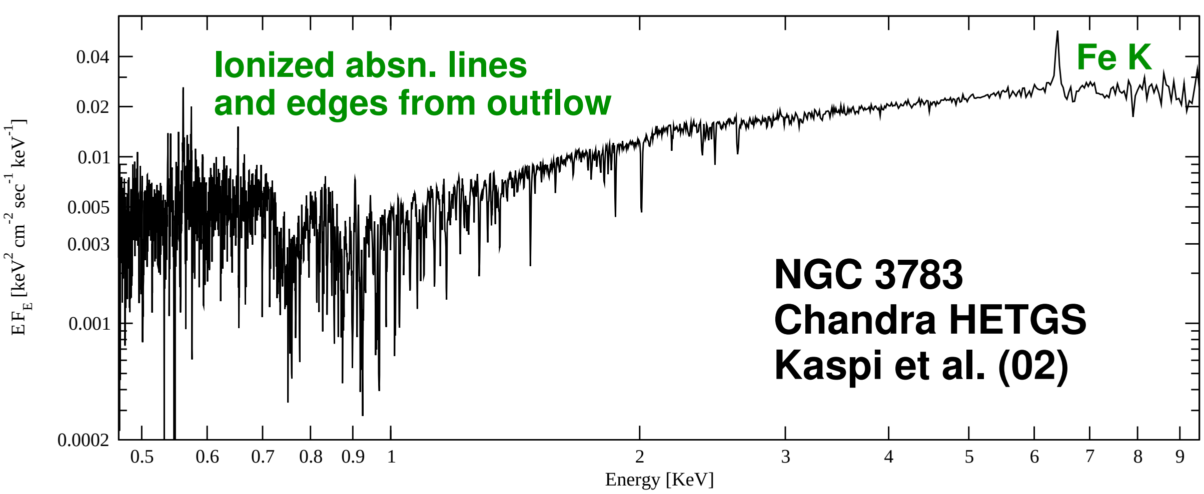

Also unidentified features

Also substantial jet–linked X–rays in radio–loud AGN

Reduced Absorption Bias

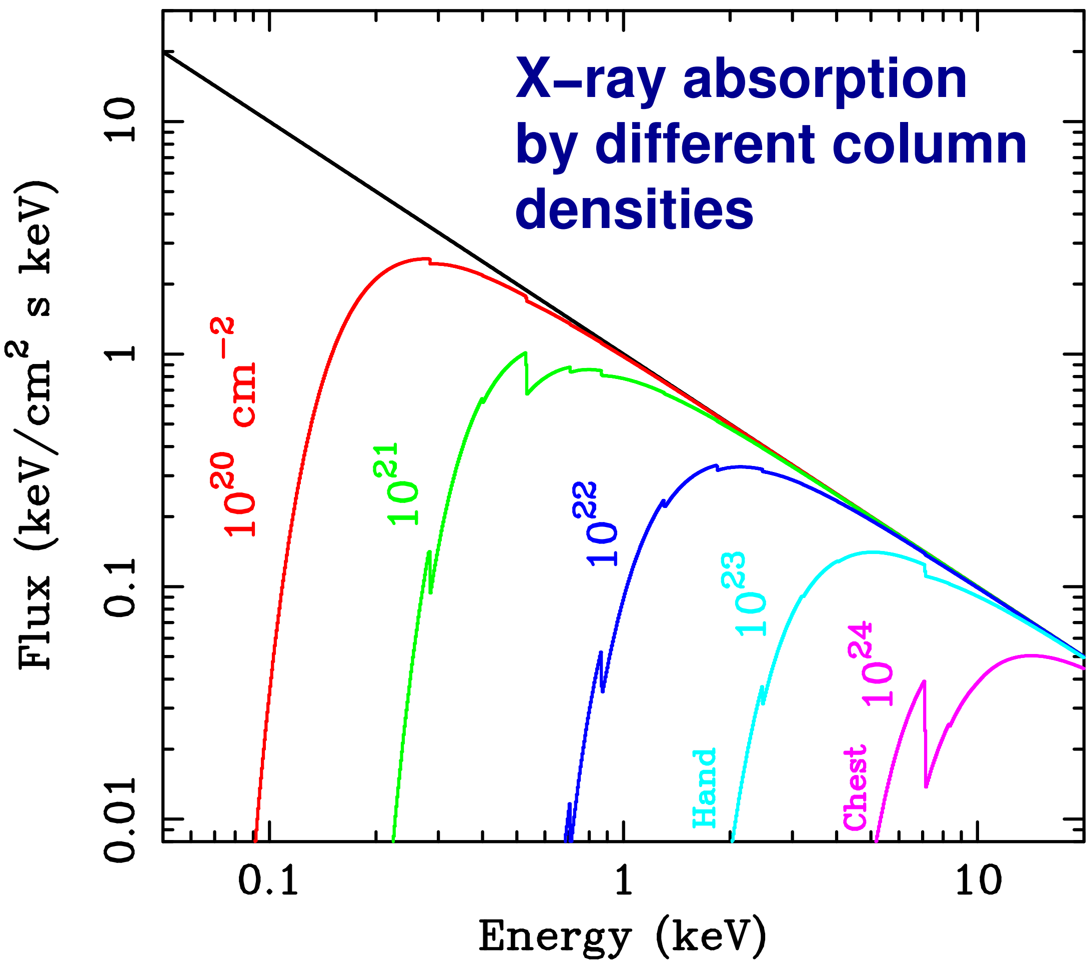

X–ray absn. sensitive to huge range of columns

Absn. bias drops further going to high redshift

Minimal Dilution by Host–Galaxy Light

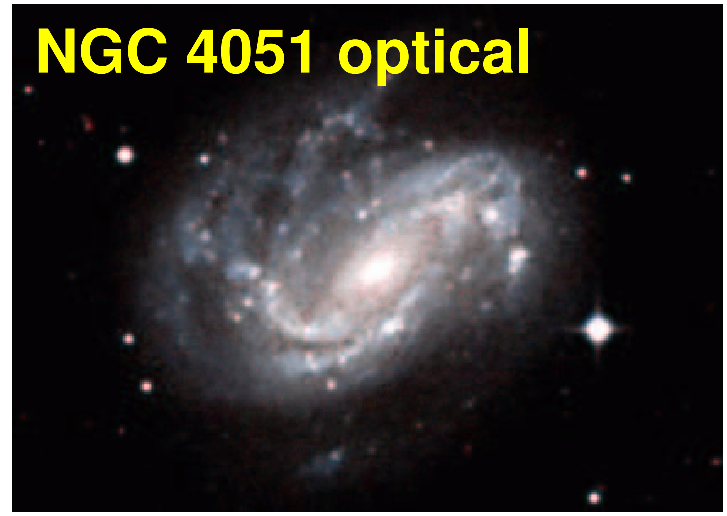

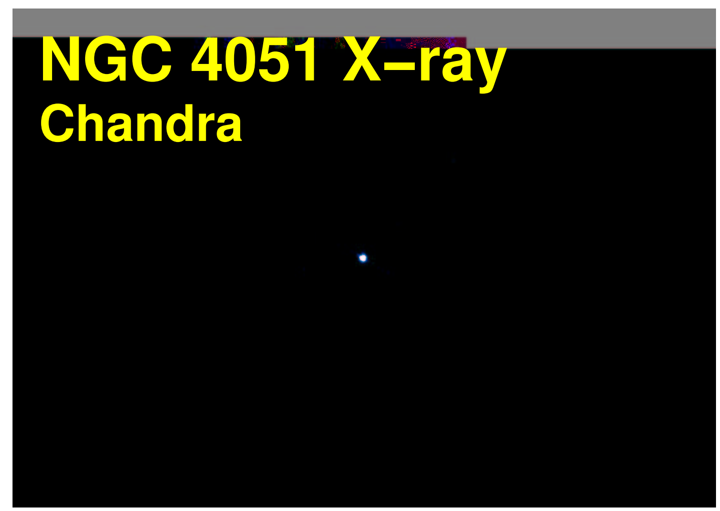

Even more important for obsc. AGN

These two effects largely responsible for great effectiveness of X–ray surveys in finding AGN.

Rapidly Improving Observational Capabilities

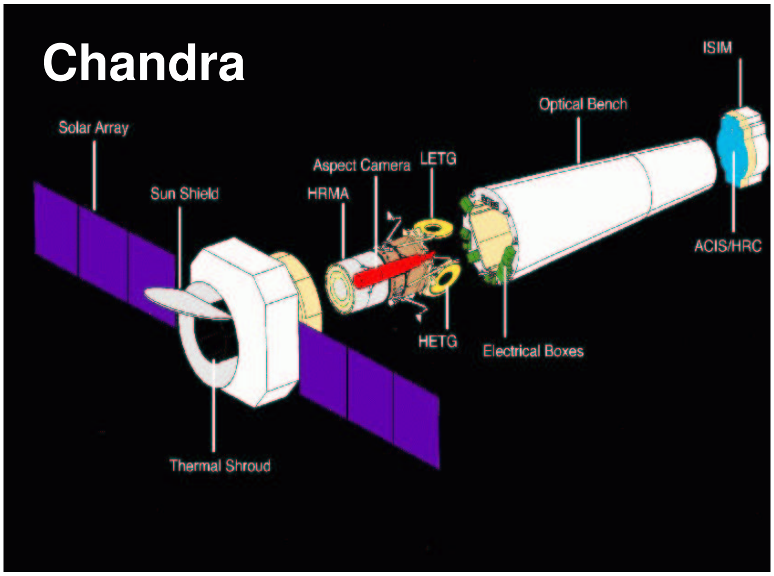

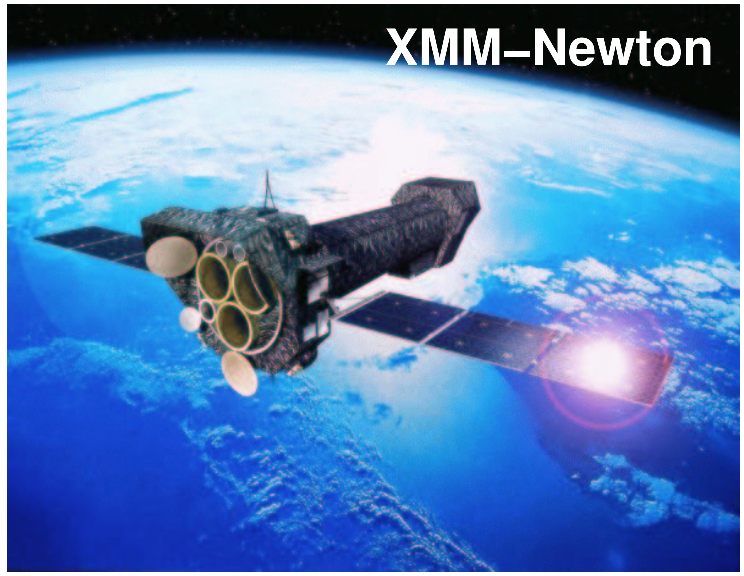

Ang. resolution and positions improved by factor ~ 10

Photon collecting ability improved by factor ~ 10

50−250 times sens. of previous missions

Spectral resolution with gratings improved by factor ~ 30−50

Well−Maintained Data Archives

Large−scale investigations with direct access to all data for calibration control etc.

Students can begin extensive projects without the need to spend years building up reservoirs of data.

The Chandra Deep Field–North

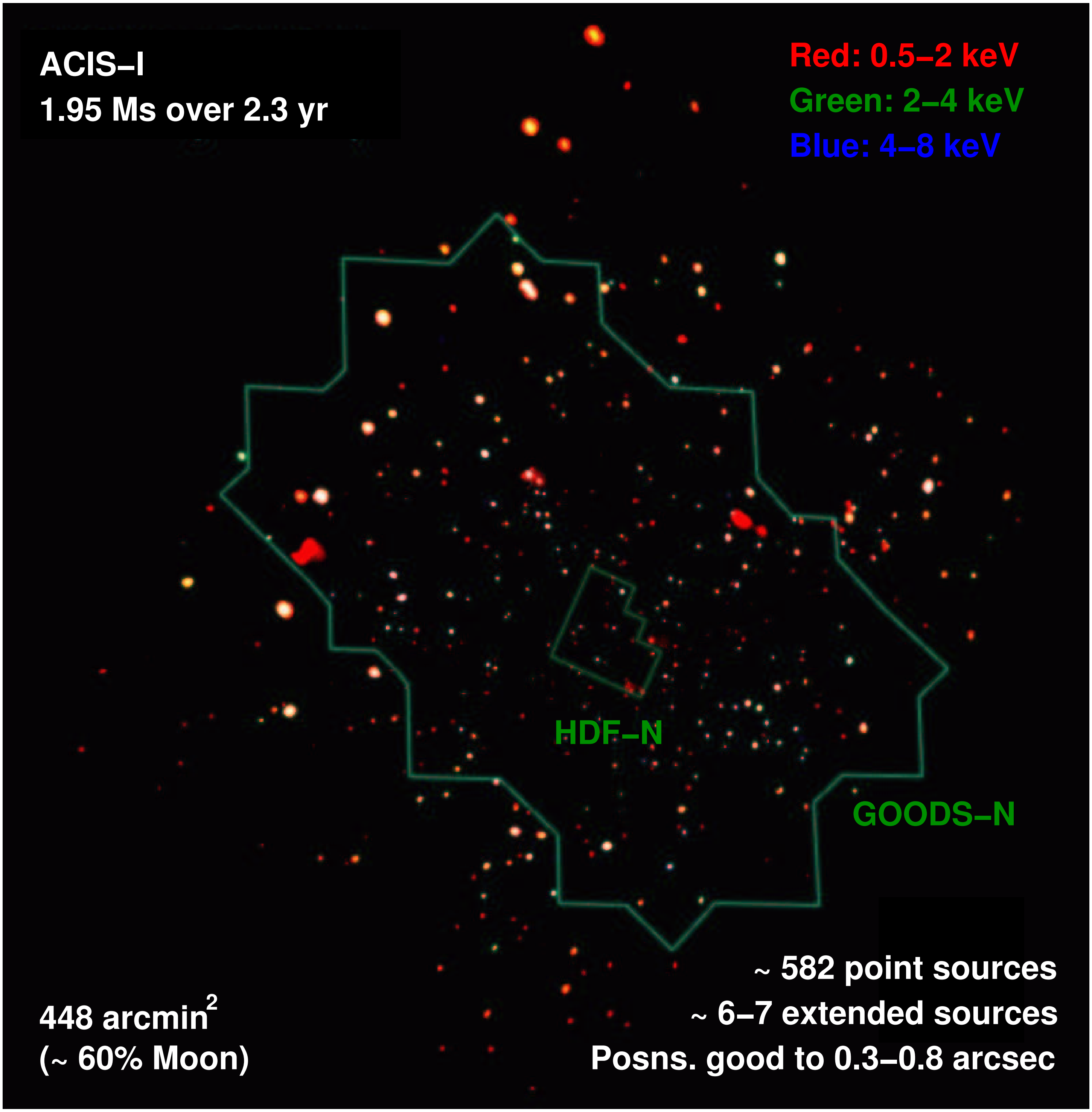

50–250 times the sensitivity of pre–Chandra surveys and still photon limited near the aim point.

Ongoing Chandra and XMM–Newton Surveys

21 Ongoing Deep Surveys

Survey Name	Exposure	Representative Reference or Note
	Chandra	
Chandra Deep Field-North	1950 ks	D.M. Alexander et al., 2003, AJ, 126, 539
Chandra Deep Field-South	940 ks	R. Giacconi et al., 2002, ApJS, 139, 369
HRC Lockman Hole	300 ks	PI: Murray
Extended CDF-S	250 ks	PI: Brandt
Groth-Westphal	200 ks	PI: Nandra
Lynx	185 ks	D. Stern et al., 2002, AJ, 123, 2223
LALA Cetus	177 ks	PI: Malhotra
LALA Boötes	172 ks	J.X. Wang et al., 2004, AJ, 127, 213
SSA13	101 ks	A.J. Barger et al., 2001, AJ, 121, 662
3C295	100 ks	V. D'Elia et al., 2004, astro-ph/0403401
Abell 370	94 ks	A.J. Barger et al., 2001, AJ, 122, 2177
SSA22 "protocluster"	78 ks	L.L. Cowie et al., 2002, ApJ, 566, L5
ELAIS	75 ks	J.C. Manners et al., 2003, MNRAS, 343, 293
WHDF	75 ks	PI: Shanks
	XMM-Newton	
Lockman Hole	766 ks	G. Hasinger et al., 2001, A&A, 365, L45
Chandra Deep Field-South	317 ks	A. Streblyanska et al., 2004, astro-ph/0309089
13 hr Field	200 ks	M.J. Page et al., 2003, AN, 324, 101
Chandra Deep Field-North	180 ks	T. Miyaji et al., 2003, AN, 324, 24
Subaru Deep	100 ks	PI: Watson
ELAIS S1	100 ks	PI: Fiore
Groth-Westphal	80 ks	T. Miyaji et al., 2004, astro-ph/0402617

The Extended *Chandra* Deep Field-South is comprised of four fields (each 250 ks), the *XMM-Newton* ELAIS S1 survey is comprised of four fields (each 100 ks), and the *Chandra* ELAIS survey is comprised of two fields (each 75 ks). The *XMM-Newton* Subaru Deep survey also has seven flanking fields (each ≈ 50 ks). Only the first ≈ 100 ks of the *XMM-Newton* Lockman Hole data have been published at present.

~ 3.5 sq. degrees in total

18 Ongoing "Wide" Surveys

Survey Name	Ω (deg^2)	Representative Reference or Note
	Chandra	
ChaMP	14	D.W. Kim et al., 2004, ApJS, 150, 19
Clusters Serendipitous	1.1	P. Gandhi et al., 2004, MNRAS, 348, 529
CYDER	...	F.J. Castander et al., 2003, AN, 324, 40
Lockman Hole NW	0.4	A.T. Steffen et al., 2003, ApJ, 596, L23
MUSYC	1	PI: van Dokkum
NOAO DWFS	9.3	PI: Jones
SEXSI	2.2	F.A. Harrison et al., 2003, ApJ, 596, 944
SWIRE Lockman	0.6	PI: Wilkes
1 hr Field	0.2	PI: McHardy
13 hr Field	0.2	I.M. McHardy et al., 2003, MNRAS, 342, 802
	XMM-Newton	
AXIS	...	X. Barcons et al., 2002, A&A, 382, 522
CFRS	0.6	T.J. Waskett et al., 2003, MNRAS, 341, 1217
HBS28	9.8	A. Caccianiga et al., 2004, A&A, 416, 901
HELLAS2XMM	2.9	A. Baldi et al., 2002, ApJ, 564, 190
LSS	64	M. Pierre et al., 2004, astro-ph/0305191
Survey Science Center	...	M.G. Watson et al., 2001, A&A, 365, L51
VIMOS	2.3	PI: Hasinger
2dF	1.5	A. Georgakakis et al., 2003, MNRAS, 344, 161

The second column above lists estimated survey solid angles; survey sensitivities are not uniform but rather vary significantly across these solid angles. In some cases, survey solid angles are not well defined and thus are not listed. In these cases, the reader should consult the listed reference or note for further details.

Lists above available from astro–ph/0403646

X-ray Source Classification Challenges

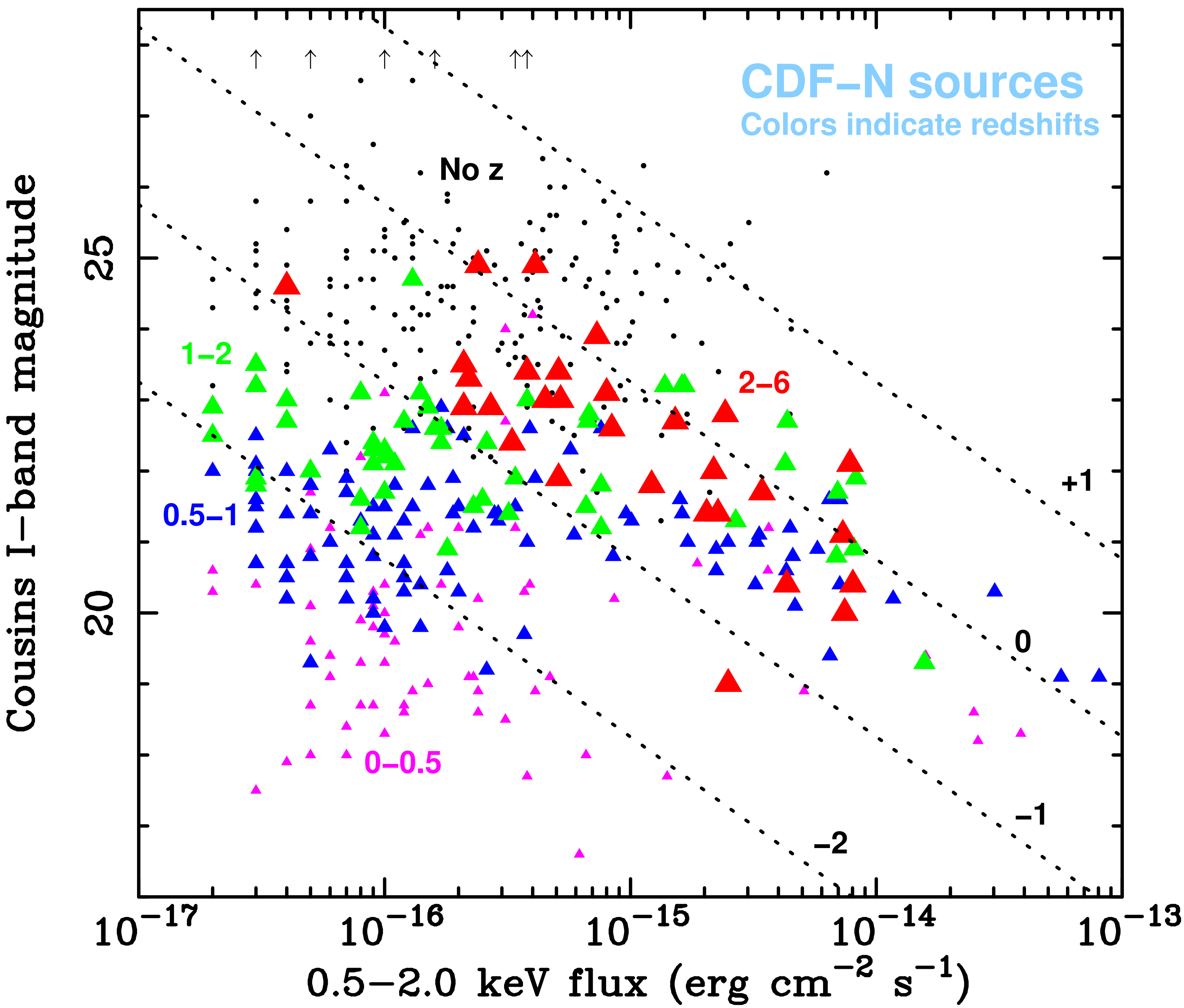

Many sources too faint for efficient spectroscopy.

50-70% spectroscopic completeness for deepest Chandra & XMM-Newton fields.

Many have modest apparent optical luminosities, so signif. host-galaxy dilution in a spectroscopic aperture.

"Schism" between optical and X-ray classification schemes.

Optical Type 1 / 2 versus X-ray unobscured / obscured.

Broad diversity of source types.

Extragalactic X–ray Source Types

Hubble Deep Field–North

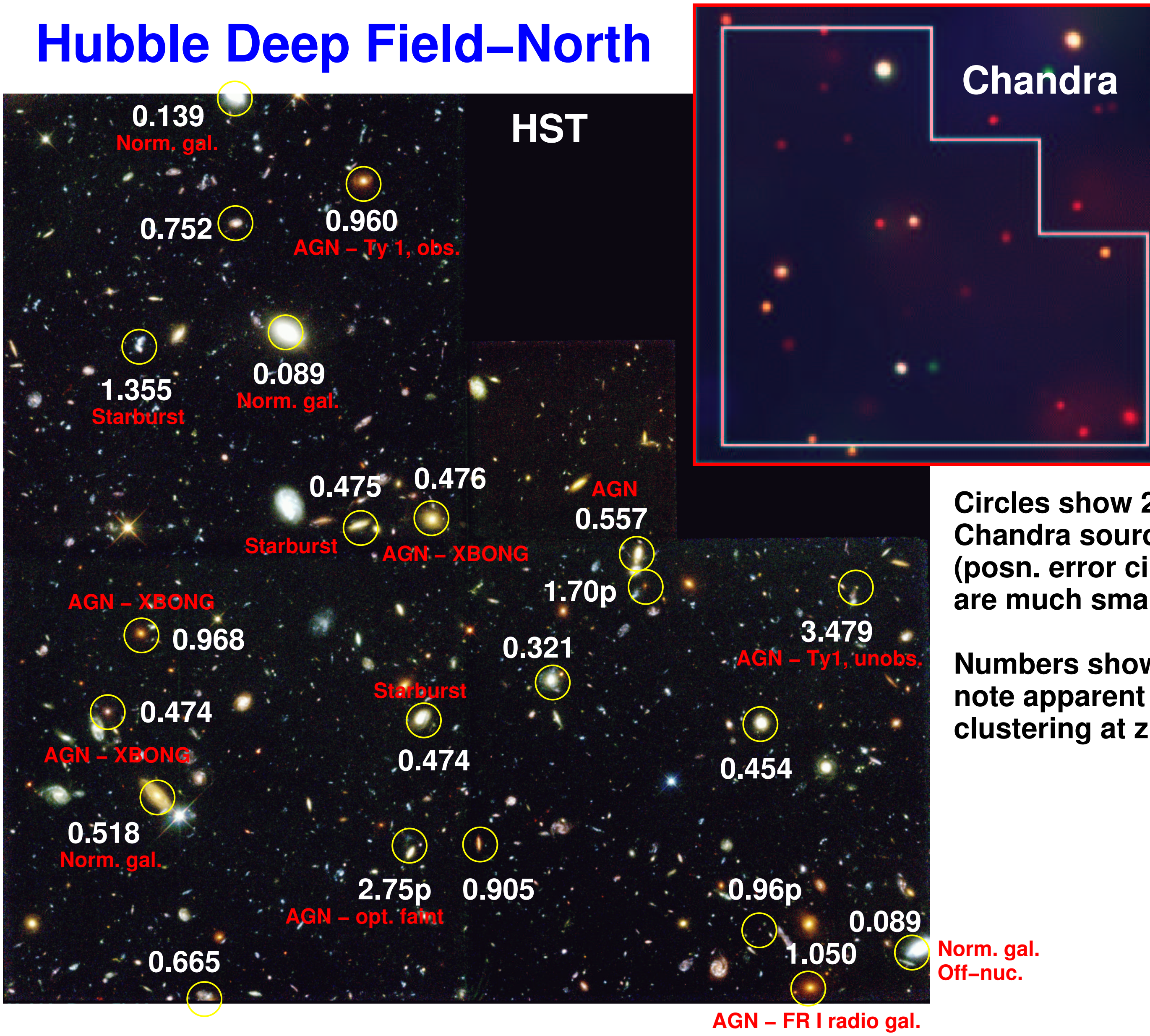

Circles show 2 Ms Chandra sources (posn. error circles are much smaller)

Numbers show redshifts; note apparent redshift clustering at z ~ 0.475

Unobscured and obscured AGN
Optically faint X–ray sources
X–ray Bright, Optically Normal galaxies (XBONGs)
Starburst and "normal" galaxies
Groups and clusters

AGN dominate the number counts; get ~ 7000 deg^{-2}

- Higher than optical spectroscopic selection by factor ~ 10
- Reduced obscuration bias
- Minimal host–galaxy dilution in X–rays

Extragalactic Chandra Deep Field Number Counts by Source Type

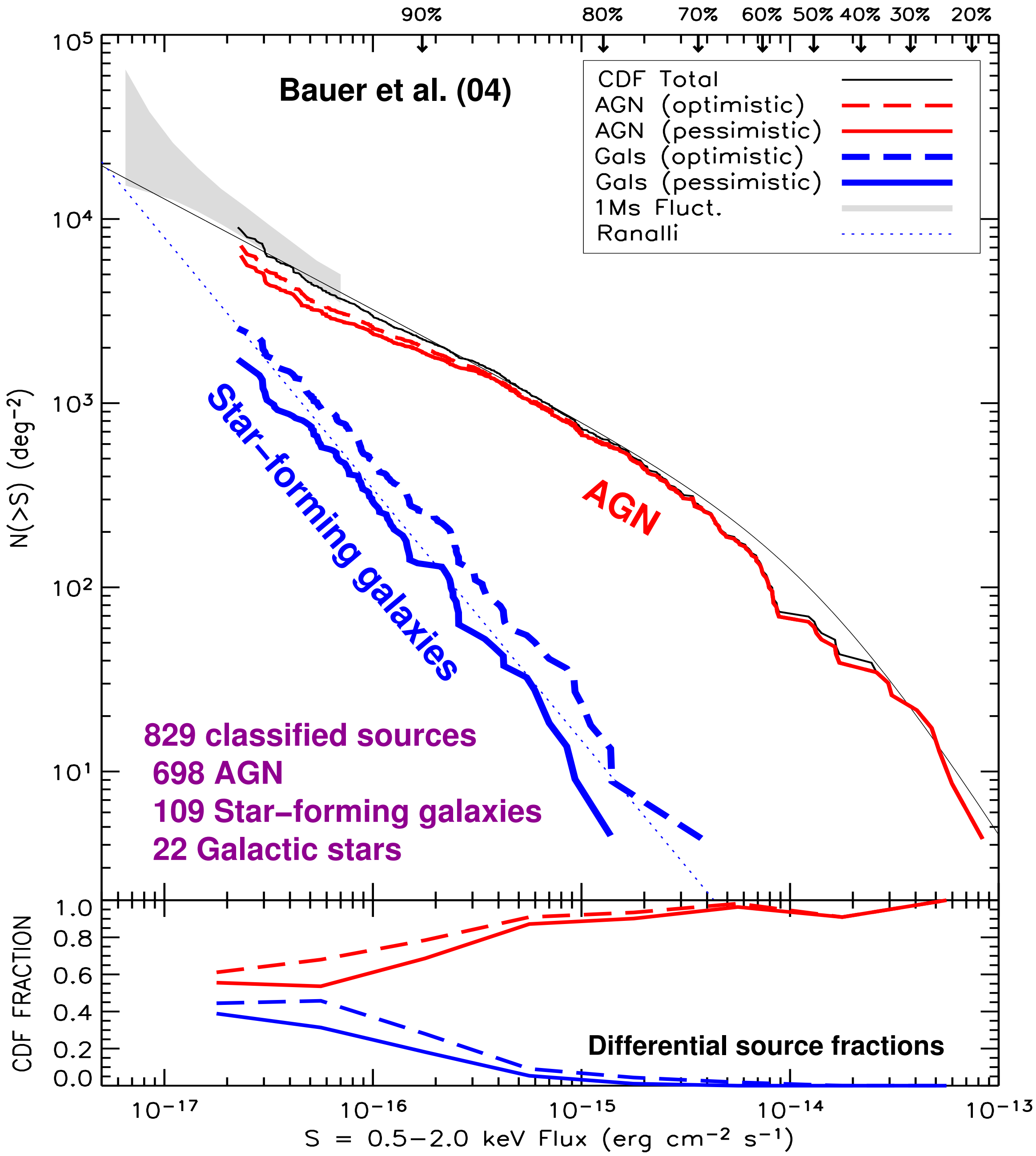

Classifications based upon

- X–ray luminosities and spectral properties
- X–ray–to–optical flux ratios
- Optical spectra
- Radio morphologies and spectra

Deep–Field Luminosities and Redshifts

Most deep–field sources have luminosities comparable to local Seyferts – could see these to z ~ 6–10.

Most of XRB made by moderate–lum. objects at z < 2

Type 2 quasars etc. make only small contribution.

Some incompleteness bias, but real low–z enhancement compared to expectations.

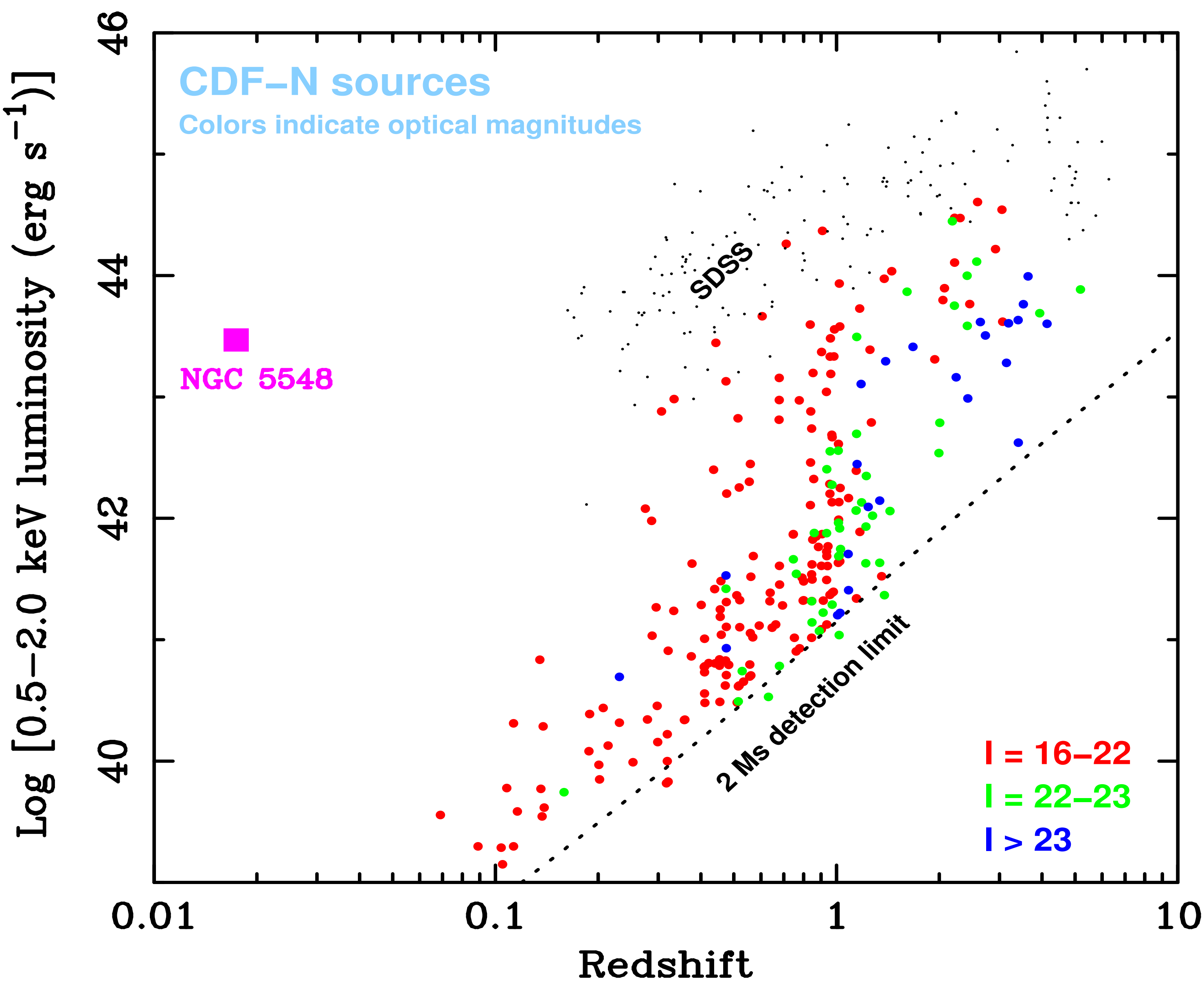

Completeness of X–ray AGN selection good relative to methods at other wavelengths – only 1–2 AGN missed in CDF–N.

Problem of Compton–thick AGN at z > 0.5–2.

AGN like NGC 1068, NGC 6240, Mrk 231 will still be missed.

Number Density Evolution with Redshift

X–ray surveys allow the evolution of lower–luminosity AGN to be studied (relative to optical quasar surveys).

Lower–luminosity AGN do not evolve as strongly with redshift as quasars, and they "peak" at lower redshift.

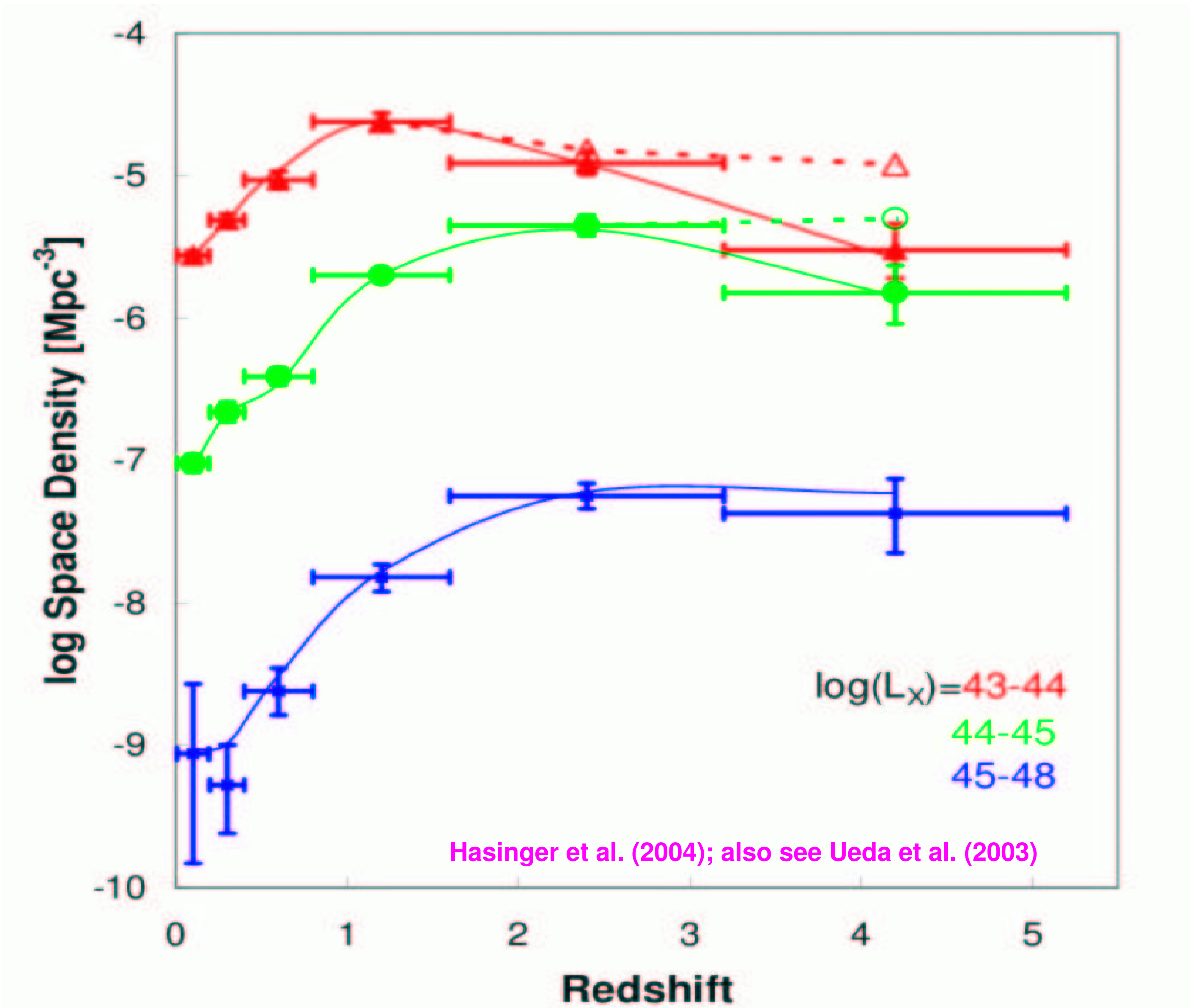

Incompleteness of

Optical follow–up

AGN X–ray selection

at high redshift remain significant error sources.

X–ray AGN in Submillimeter Galaxies

How many of these young, forming galaxies contain actively accreting SMBH? Are SMBH energetically important?

X–rays are useful AGN diagnostic for opt. faint SCUBA sources – majority population otherwise difficult to investigate.

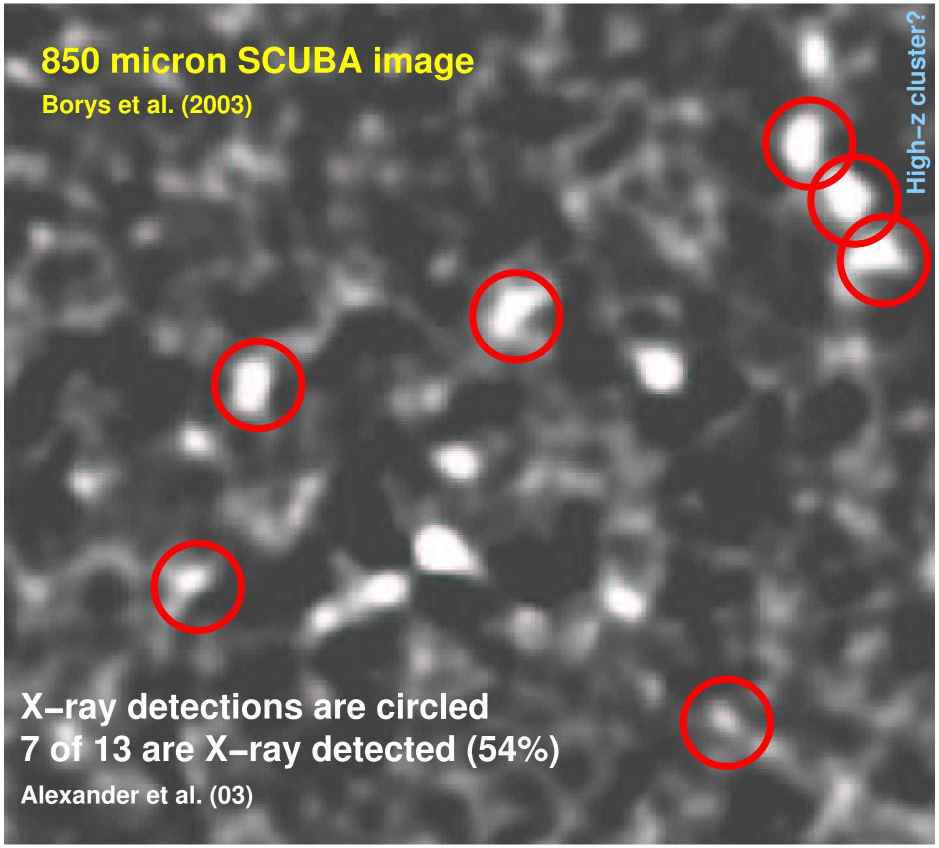

With 2 Ms exposure get large X–ray / SCUBA overlap, unlike ~ 20–150 ks exposures.

About 70% of X–ray detected appear to contain AGN.

Remaining 30% may be X–ray detected starbursts.

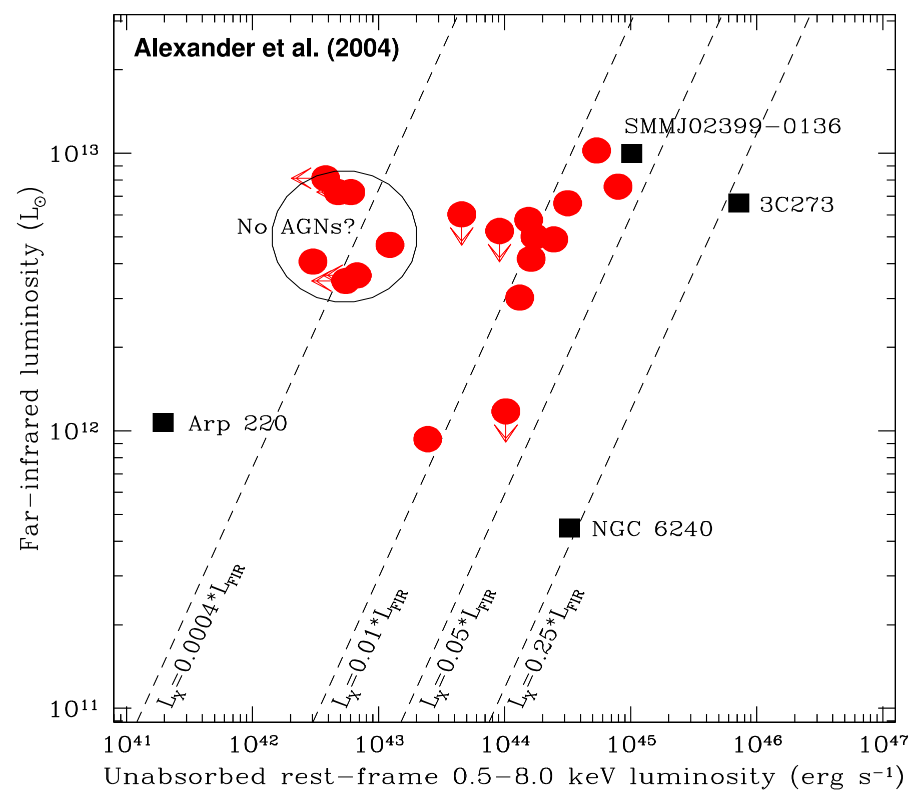

After modeling X–ray absn., likely AGN have X–ray luminosities comparable to Seyfert galaxies.

Comparison with local objects indicates the AGN contribute ~ 20% or less of total luminosity.

So star formation likely dominates energy budget.

X–ray Constraints on z > 4 AGN Demography and Physics

z > 4 AGN and AGN Candidates in CDF–N

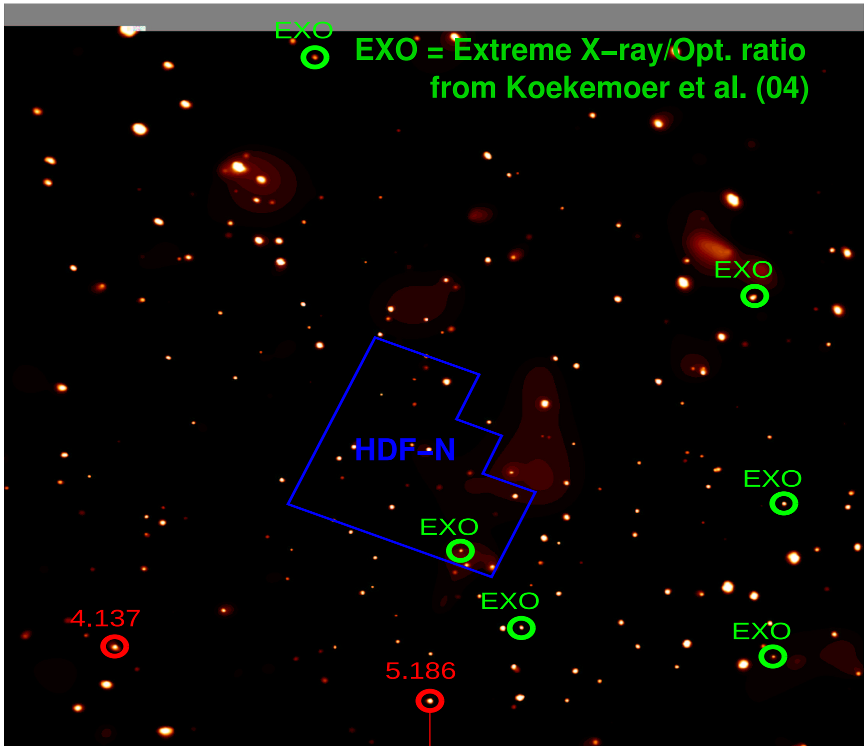

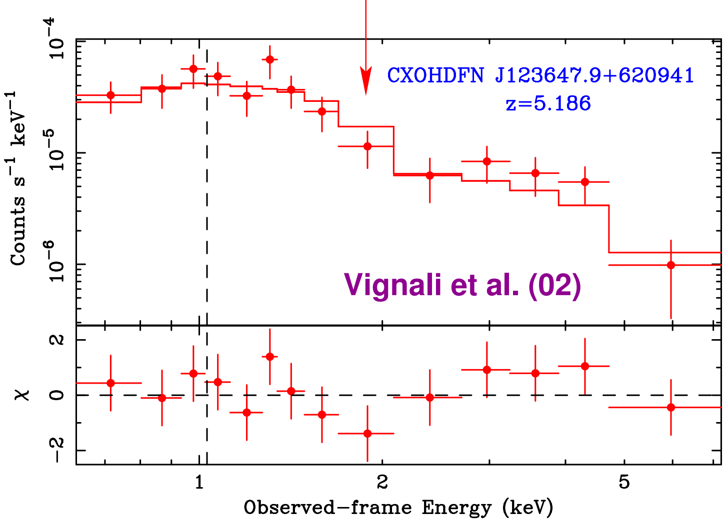

Probe moderate–lum., typical AGN at z > 4

Minimize absn. bias (rest–frame 20–40 keV)

Find or constrain sky dens. exploiting Lyman break.

Alexander et al. (01), Barger et al. (03), Cristiani et al. (04), Koekemoer et al. (04)

3 AGN confirmed at z > 4 in CDFs.

Several others in moderate–depth Chandra fields.

Stacking analyses constrain average AGN content of high–redshift populations.

X–ray Stacking of GOODS Lyman Break Galaxies

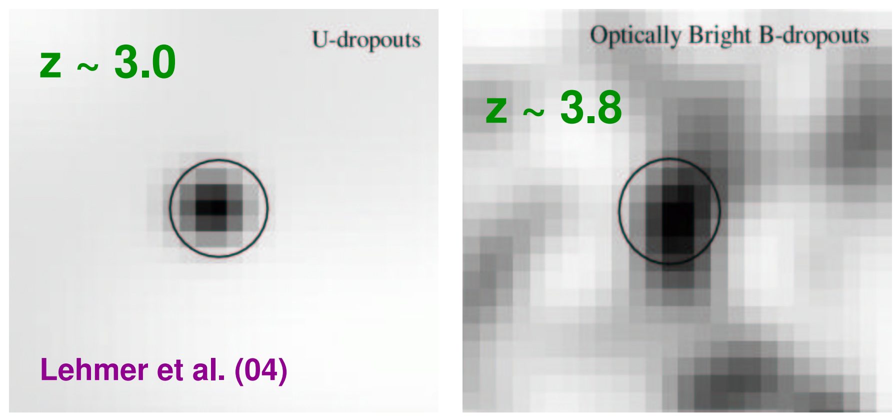

Constraining Cosmic Evolution of Quasar X–ray Emission

4–10 ks Chandra snapshots allow efficient X–ray detections at z = 4–6.5.

Now > 100 detections obtained.

Highest z SDSS, PSS+BRI, RLQs, Exotic

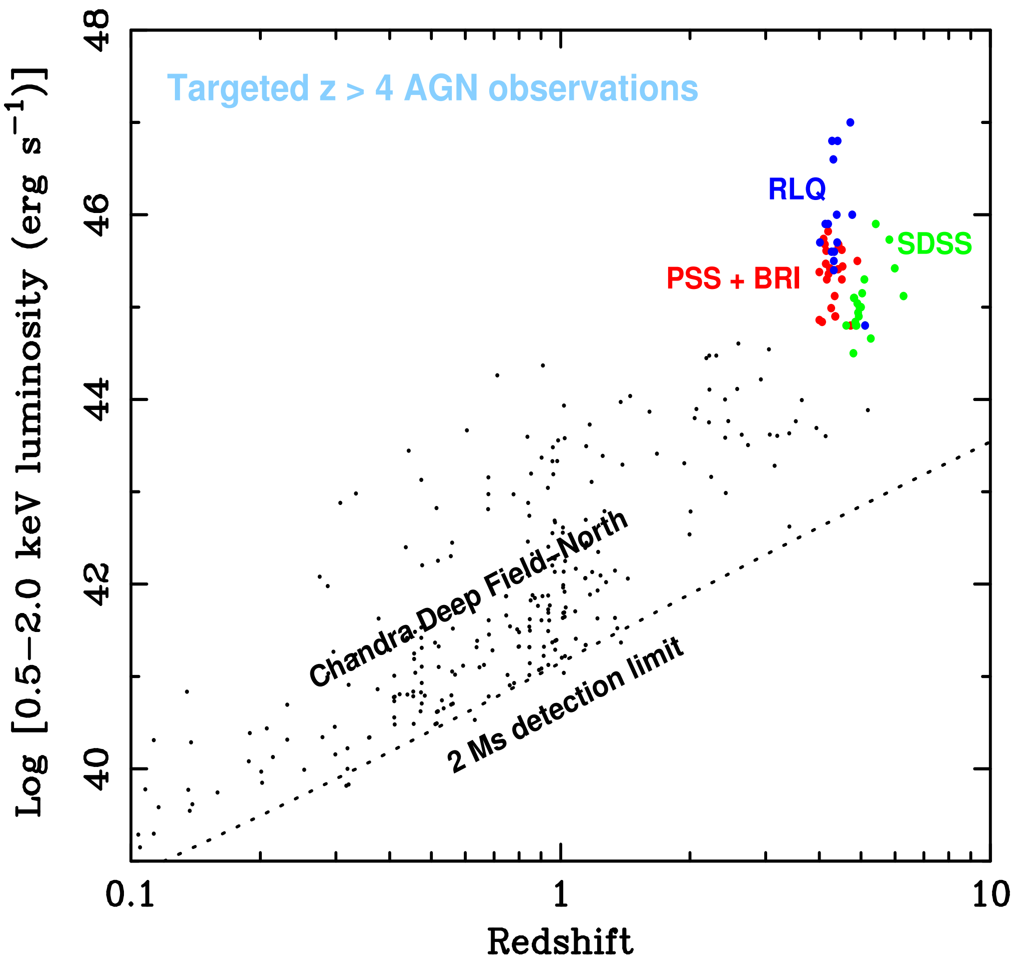

X–ray flux, lum., continuum shape, absorption, extent, α_{ox}

Combine with well–defined, lower z samples to constrain X–ray evolution.

Want broad lum. and redshift coverage.

RQQ vs. RLQ separation, BAL removal, high detection fraction (avoid pattern censoring)

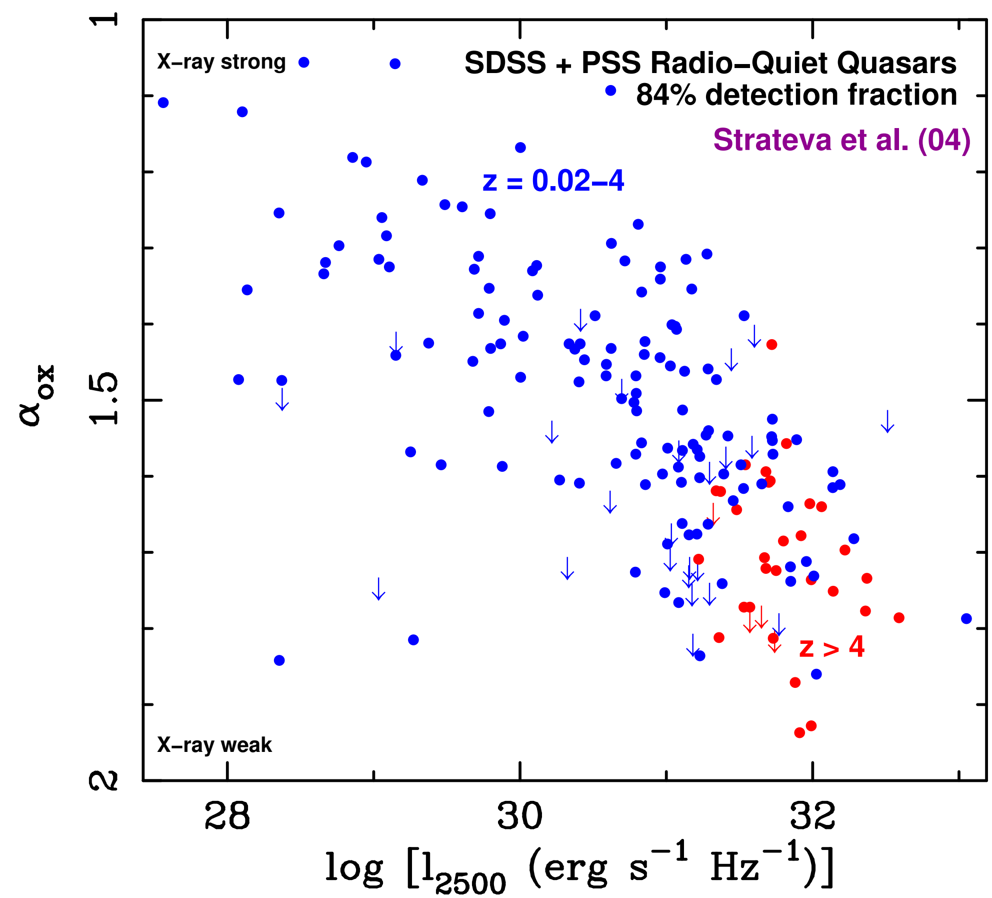

Partial correln. analyses of ~ 152 SDSS+PSS RQQs spanning z = 0.02–6.28 indicate lum. effect is primary.

Also see Vignali, Brandt, & Schneider (03)

X–ray Spectroscopy at High Redshift

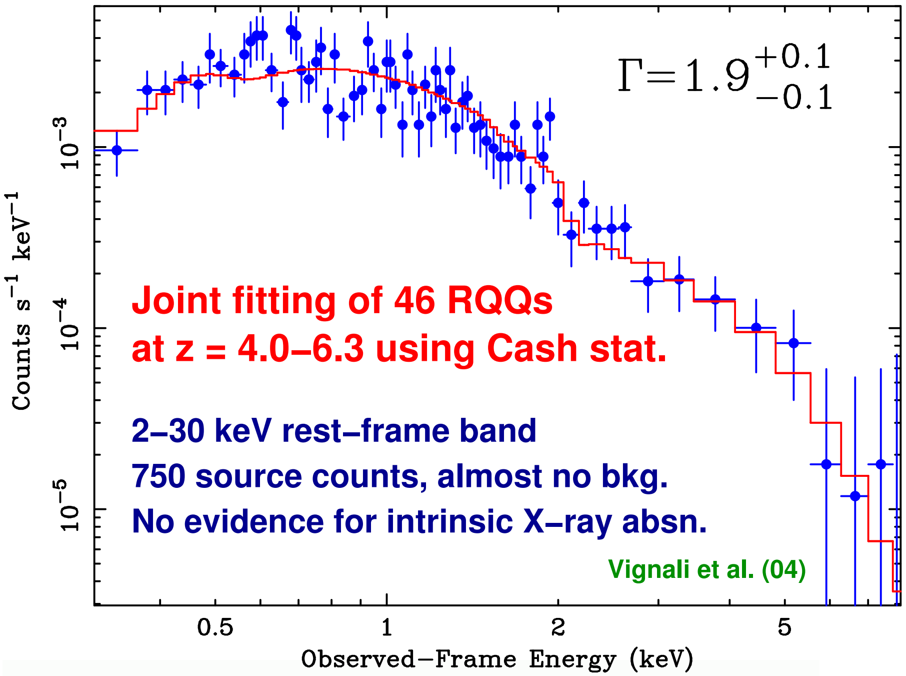

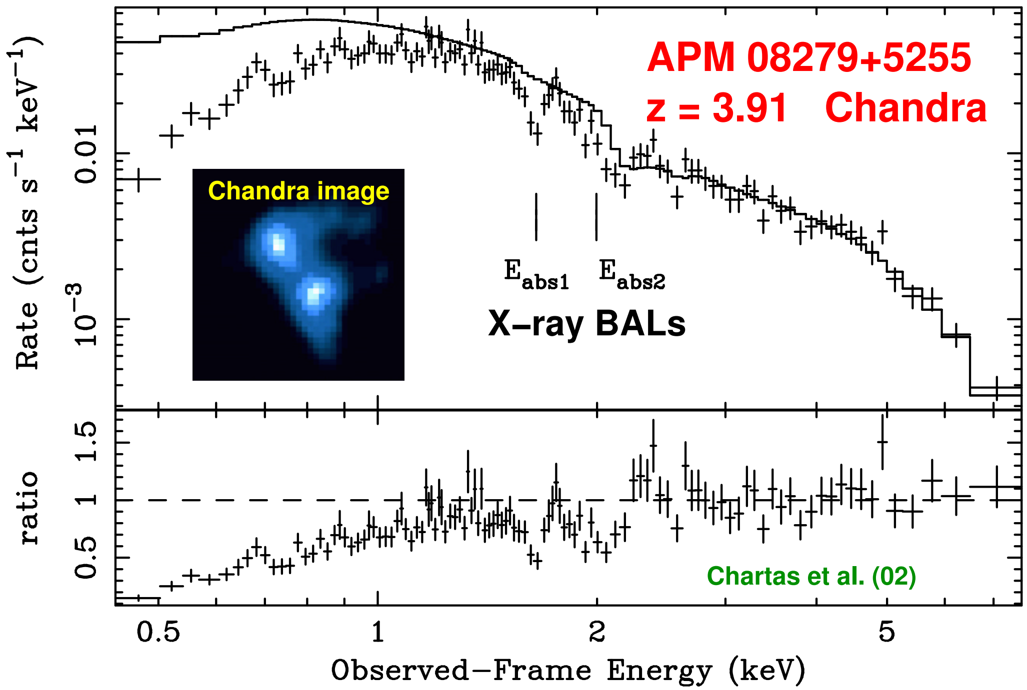

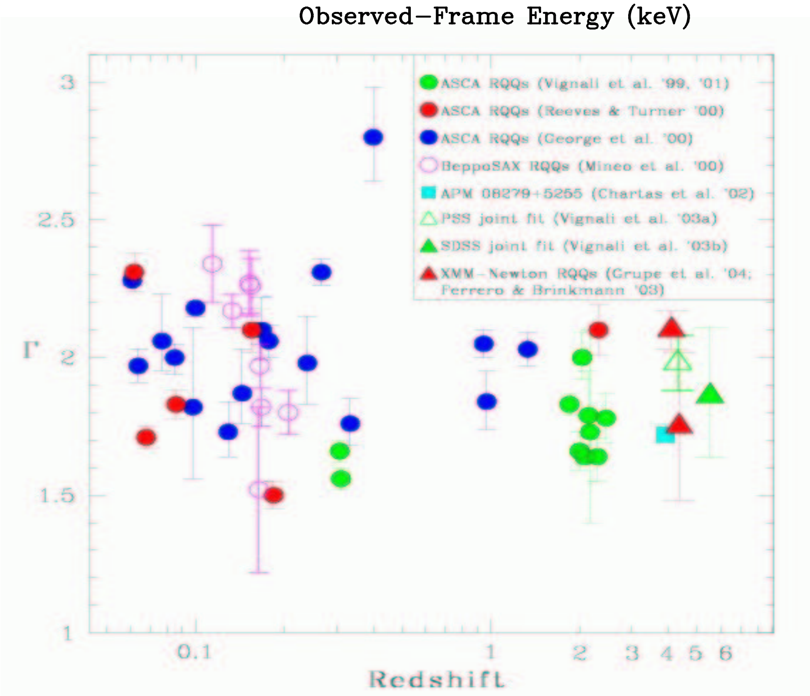

Active galaxies at z ~ 4–6 and z ~ 0–2 have reasonably similar X–ray and broad–band spectra. No hints of greatly different accretion / growth mechanisms.

(After controlling for luminosity effects)

Small–scale X–ray emission regions insensitive to strong large–scale environmental differences from z ~ 0–6. X–ray emission appears universal, even at z ~ 4–6.

Helps to validate results from X–ray surveys.

Some Future Prospects – X–ray Surveys and Constellation–X

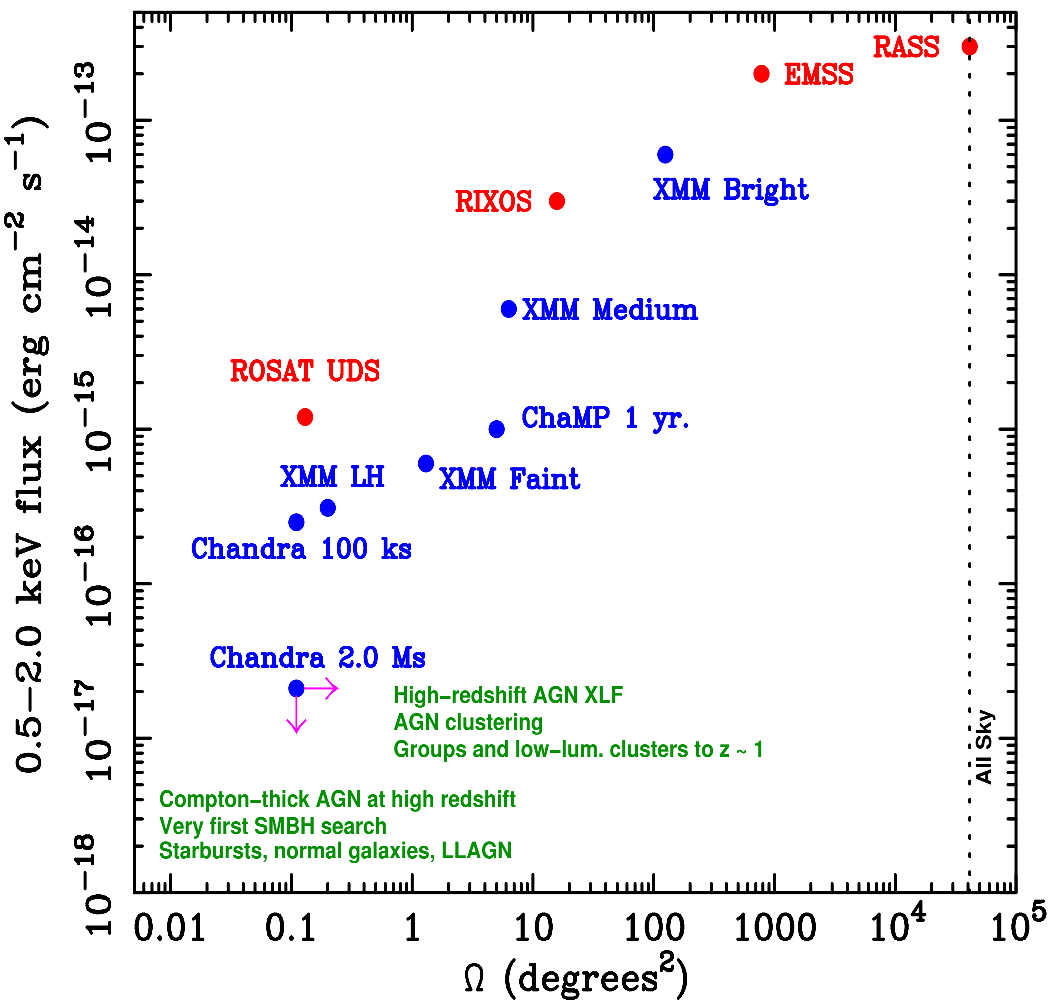

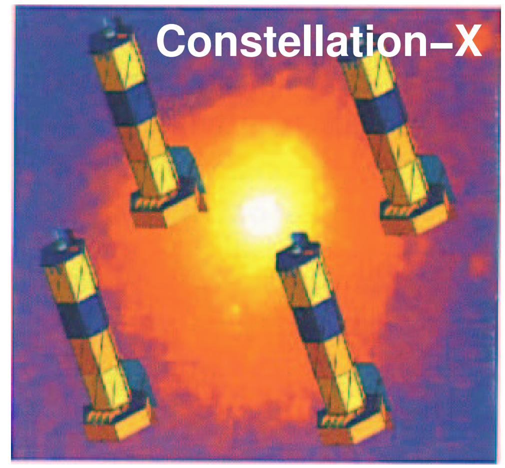

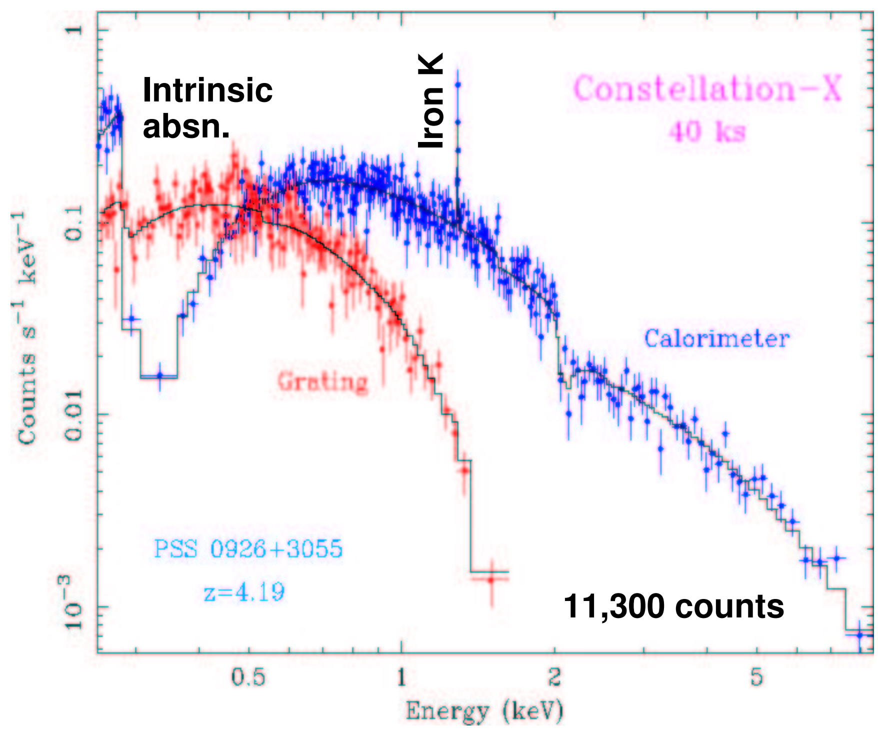

Chandra can go significantly deeper and wider with best positions for ~ 20 yr.

Many superb targets for snapshot and spectroscopic observations with Chandra and XMM–Newton.

X–ray Detectability of Proto–Quasars and Black Holes from the First Stars